

Corrosion Behaviors of SS316 and Ni-base Alloys in Molten LiCl-KCl Salt at High Temperature

Jun Woo Park, Jong-Il Yun*

Department of Nuclear and Quantum Engineering, KAIST, Korea

*Corresponding author: jiyun@kaist.ac.kr

1. Introduction

Molten salt reactor (MSR) utilizing molten salts as a coolant at high temperature is one of the promising advanced reactor types. Due to the high melting point (>300°C) and boiling point (>1400°C) of molten salts, a higher thermal efficiency can be achieved, and the operation under normal pressure is possible. In addition, the negative temperature coefficient can be obtained, and decay heat can be dissipated efficiently.

Various types of salts, such as fluoride and chloride salts, are considered as coolants in MSR. The fluoride salt-based MSR, called MSRE, was built and operated at Oak Ridge National Laboratory (ORNL) in the 1960s, but the chloride salt-based MSR has not yet been built. However, it is known that chloride salts are the proper salt for fast spectrum reactor, which can consume used fuels from light water reactors (LWRs) [1]. Therefore, much attention has been paid to the chloride salt-based MSR recently.

One of the main challenges in MSR is the compatibility of salts with structural materials. Nuclear fuels and fission products are involved in the coolant (salts) in MSR at high temperature, unlike typical LWRs, so the corrosion of structural materials can be accelerated. The corrosion behavior of structural materials in fluoride salts has been extensively investigated during operation of the MSRE. On the other hand, there is a lack of knowledge about the corrosion of structural materials under various conditions of chloride salts.

In this study, therefore, the corrosion behavior of candidate structural materials in chloride salts at high temperature was investigated. SS316 and Ni-based alloys such as Alloy 617 and Hastelloy N, which are widely used as corrosion-resistance materials at high temperature, were selected as structural material candidates. In addition, LiCl-KCl eutectic salt was chosen as the molten salt, the properties of which are well-known due to its use in pyroprocessing. The phase change and surface change of structural materials were analyzed by X-ray diffraction (XRD) and scanning electron microscope (SEM). In addition, electron backscatter diffraction (EBSD) analysis was applied to obtain the grain orientation information.

2. Experimental

Anhydrous LiCl-KCl (99.99%, LiCl 44wt%, Sigma-Aldrich) eutectic salt was utilized in this experiment. The salt was dried at 300°C for 10 hours to remove residual moisture before melting. In this study, samples of SS316,

Alloy 617, and Hastelloy N with a geometry of 5.0mm×10.0mm×1.5mm were used. The chemical compositions of the alloys used were analyzed by inductively coupled plasma-optical emission spectroscopy (ICP-OES) and are listed in Table I. All specimens were ground up to 2000 grit SiC paper and polished with 0.05µm alumina suspension.

Table I: Chemical compositions of alloys used (wt%)

	SS316	Alloy 617	Hastelloy N
Ni	10.7	51.7	70.8
Cr	17.3	22.9	7.3
Mo	2.0	9.5	16.6
Fe	68.2	1.1	4.3
Co	-	13.1	-
Si	0.7	0.2	0.3
Mn	1.0	1.0	0.5
C	0.07	-	0.06

All corrosion experiments were conducted in the Ar-filled (99.999%) glovebox, where the oxygen and H₂O concentrations are controlled below 5ppm. The experimental temperature was maintained at 500±5°C by an electrical furnace attached under the glovebox. Quartz cells were utilized as sample containers. After corrosion experiments, corroded samples were cleaned with ethanol and deionized water to remove residual salt on the surface of the samples.

3. Result and Discussion

The XRD analysis was performed before and after the corrosion test for 100 hours at 500°C. Fig. 1 represents the XRD results of three different alloys. Characteristic γ -phase peaks of FCC structure appear commonly for all alloys before and after corrosion, and the minor martensite impurity peaks are observed in the SS316 specimen prior to corrosion. It is obvious that there is no significant change in the XRD results before and after the corrosion. The change in the XRD results of structural materials has been reported at more than 700°C, which corresponds to harsher conditions [2]. Therefore, the experimental conditions in this study (500°C) are not such extreme conditions that can induce the phase change of structural materials.

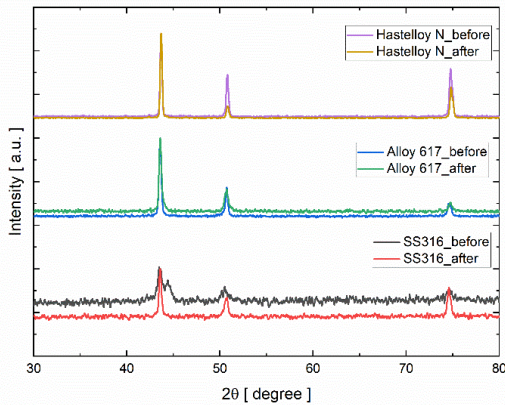


Fig. 1. XRD results of SS316, Alloy 617, and Hastelloy N before and after 100 hours corrosion in LiCl-KCl at 500°C

The corroded surface of each alloy was analyzed by SEM and EBSD. Fig. 2(a) and 2(b) show the SEM and EBSD results of SS316 corroded in LiCl-KCl at 500°C for 100 hours and 200 hours, respectively. Although there is no significant phase change, the corroded surface is observed. The 100 hour corroded specimen does not show extensive dissolution behavior, but certain grains suffer from the higher dissolution rate in the 200 hour corroded specimen. The EBSD analysis performed on the same region of the SEM image indicates that the dissolution appears strongly when grains are close to $\{111\}$ planes and far away from $\{001\}$ planes.

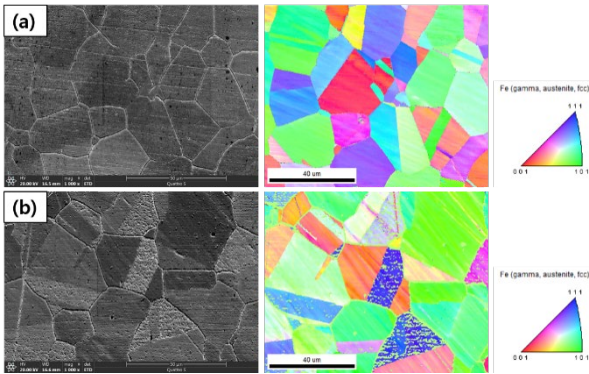


Fig. 2. SEM and EBSD results of SS316 (a) after 100 hour corrosion and (b) 200 hour corrosion in LiCl-KCl at 500°C

The SEM and EBSD results of Alloy 617 are shown in Fig. 3. Grains close to $\{001\}$ planes show the smooth surface compared to other grains, whose surface is rough. The roughness of the corroded surface is high for the grains close to $\{111\}$ planes.

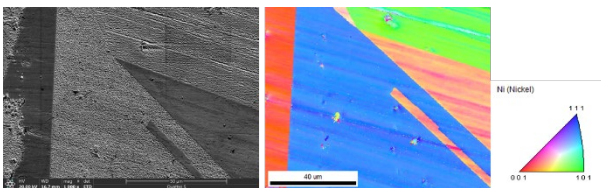


Fig. 3. SEM and EBSD results of Alloy 617 after 100 hour corrosion in LiCl-KCl at 500°C

The surface analysis by SEM and EBSD is also conducted for Hastelloy N, as shown in Fig. 4. Grains with the smooth surface are close to $\{001\}$ planes and grains with the rough surface are close to $\{111\}$ planes based on the EBSD results, such as SS316 and Alloy 617

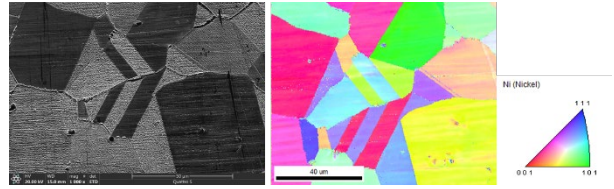


Fig. 4. SEM and EBSD results of Hastelloy N after 100 hour corrosion in LiCl-KCl at 500°C

The dissolution behavior becomes severe in grains close to $\{111\}$ planes for all alloys. On the other hand, grains close to $\{001\}$ planes show less dissolution. Grain orientation-dependent dissolution behavior has also been reported in other aqueous systems [3,4]. The first to consider is the surface energy of the plane. The surface energy of the plane can be simply expressed as equation (1),

$$SE = 2 \frac{2|h|+|k|}{\sqrt{h^2+k^2+l^2}} \times \frac{E_b}{d^2} \quad (1)$$

where h , k , and l are the Miller indices ($h > k > l$), E_b is the bonding energy, and d is the bonding length [3,4]. Only h , k , and l values have to be considered in the same materials, so the surface energy of the plane is of the order $\{101\} > \{001\} > \{111\}$.

Planes with lower surface energy are expected to be stable and less reactive, but experimental results indicate higher dissolution. It is reported that the adsorption of chemical species such as oxide or hydrogen on the $\{111\}$ plane of the FCC crystal is weak [5,6]. Therefore, it is presumed that the adsorption of chemical species acting as corrosion inhibitors becomes weaker for the stable $\{111\}$ plane. Interactions between corrosion inhibitors in molten salt and structural materials may determine the grain orientation-dependent corrosion behavior. The next step of this study will be the investigation to find out the types and reaction mechanisms of corrosion inhibitors in molten salts.

4. Conclusion

The corrosion behavior of SS316 and Ni-based alloys in molten LiCl-KCl salt was analyzed at 500°C in this study. Under the experimental conditions of this study, there was no significant change in the phase of structural materials, but dissolution occurs at the surface. The roughest surface was observed on the $\{111\}$ planes, and this behavior is expected to be caused by the different adsorption behaviors of chemical species on the structural materials.

Acknowledgement

This work was supported by the National Research Foundation of Korea (NRF) grant funded by the Korean government (MSIP:Ministry of Science, ICT and Future Planning) (No. NRF-2020M2D4A1070724 and NRF-2021M2C7A1A02076339) and the Circle Foundation (Republic of Korea) as the '2021 TCF Innovative Science Project'.

REFERENCES

- [1] D.E. Holcomb, G.F. Flanagan, B.W. Patton, J.C. Gehin, R.L. Howard, and T.J. Harrison, Fast Spectrum Molten Salt Reactor Options, ORNL/TM-2011/105, 2011.
- [2] L. Guo, Q. Liu, H. Yin, T.J. Pan, and Z. Tang, Excellent corrosion resistance of 316 stainless steel in purified NaCl-MgCl₂ eutectic salt at high temperature, Corrosion Science, 166, 108473, 2020.
- [3] S. Wang, and J. Wang, Effect of grain orientation on the corrosion behavior of polycrystalline Alloy 690, Corrosion Science, 85, pp.183-192, 2014.
- [4] S. Dong, X. Chen, EC. La Plante, M. Gussev, K. Leonard, and G. Sant, Elucidating the grain-orientation dependent corrosion rates of austenitic stainless steels, Materials and Design, 191, 108583, 2020.
- [5] H.-T. Liu, A.F. Armitage, and D.P. Woodruff, Anisotropy of initial oxidation kinetics of nickel single crystal surfaces, Surface Science, 114, pp.431-44, 1982
- [6] A.N. Pour, Z. Keyvanloo, M. Izadyar, and S.M. Modaresi, Dissociative hydrogen adsorption on the cubic cobalt surfaces: A DFT study, International Journal of Hydrogen Energy, 40, pp.7064-7071, 2015.